

# Graphene plasmon polaritons: Substrate effects and nonlocal response

Thomas Christensen,<sup>1,2</sup> Antti-Pekka Jauho,<sup>1,3</sup> and N. Asger Mortensen<sup>1,2,†</sup>

<sup>1</sup>Center for Nanostructured Graphene (CNG), Technical University of Denmark, DK-2800 Kgs. Lyngby, Denmark

<sup>2</sup>Department of Photonics Engineering, Technical University of Denmark, DK-2800 Kgs. Lyngby, Denmark

<sup>3</sup>Department of Micro- and Nanotechnology, Technical University of Denmark, DK-2800 Kgs. Lyngby, Denmark

<sup>†</sup>Corresponding author: asger@mailaps.org

Compiled January 14, 2019

We theoretically examine graphene plasmon polaritons (GPP) supported by a sheet of graphene sandwiched between two dielectric media. The influence of the dielectric environment on GPP's is studied within local and nonlocal descriptions of graphene's conductivity. We demonstrate that a local-response approximation invariably leads, counter-intuitively, to a substrate-independent surface plasmon frequency  $\omega_{sp}$ . On the other hand, the nonlocal description of the electron gas allows the presence of non-vertical inter-band transitions which changes the results qualitatively: the GPP's now depend on the surroundings, and the singularity in the local GPP dispersion relation is removed. © 2019 Optical Society of America

Graphene exhibits a wide range of unusual properties, and has been the subject of riveting theoretical and experimental progress in recent years. An extraordinary manifestation of the unusual optical properties is the broadband 2.3% absorption per atomic layer [1]. Furthermore, graphene shows great promise for a range of optoelectronic, photonic and plasmonic applications [2, 3]. For example, recent studies have considered theoretically [4–8] and experimentally [9] transverse magnetic (TM) graphene plasmon polaritons (GPP) in single layer graphene (SLG) as well as in bilayer graphene. The possibility for transverse electric (TE) SPPs has been discussed for free-standing graphene [8, 10]. Extensive studies have been conducted on the properties and possible applications of longitudinal plasmons in graphene [11, 12].

The longitudinal and transversal field-excitations are often collectively called as 'plasmons', even though their physical properties can be quite different. The plasmons considered here are the TM GPPs, i.e. the transverse magnetic field-excitations near the graphene plane, highly akin to the well-known surface plasmon polaritons at metal-dielectric interfaces. For a graphene sheet sandwiched between two, possibly different dielectric media, see Fig. 1, the local-response approximation for the free carrier conductivity leads to a surprising and counter-intuitive result: a substrate-*independent* divergence of the GPP dispersion relation for frequencies approaching  $\omega_{sp}$ . Alerted by the fact that we have in recent years discovered several cases in nano-optics where the local-response description yields spurious results [13–16], we examine here the consequences of a nonlocal conductivity for GPPs. As we show below, two qualitative changes occur: (i) the divergence in the dispersion law is removed, and (ii) a substrate dependence is found, as one would expect physically.

The presence of graphene in electromagnetic calculations near optical frequencies leads to additional boundary conditions (BCs) for the electromagnetic field. The

finite conductivity of graphene and its two-dimensional character in the scale of optical wavelengths allows graphene to support a pseudo-surface current term,  $\mathbf{K}$ , and a surface charge density,  $\rho_s$ , which are incorporated into BCs through

$$\mathbf{E}_{\parallel}^+ - \mathbf{E}_{\parallel}^- = 0, \quad \varepsilon_+ \mathbf{E}_{\perp}^+ - \varepsilon_- \mathbf{E}_{\perp}^- = 4\pi\rho_s, \quad (1a)$$

$$\mathbf{H}_{\perp}^+ - \mathbf{H}_{\perp}^- = 0, \quad \hat{\mathbf{n}} \times (\mathbf{H}_{\parallel}^+ - \mathbf{H}_{\parallel}^-) = 4\pi\mathbf{K}/c, \quad (1b)$$

where  $\mathbf{E}_{\parallel\perp}^{\pm}$  and  $\mathbf{H}_{\parallel\perp}^{\pm}$  are the parallel and perpendicular components of the electric and magnetic fields above and below the interface, respectively. The surface current and the surface density are interrelated by the continuity equation  $\nabla_{\parallel} \cdot \mathbf{K}(\mathbf{r}_{\parallel}, t) = -\partial_t \rho_s(\mathbf{r}_{\parallel}, t)$ . In the linear response regime  $\mathbf{K}$  is determined by the in-plane Ohmic conductivity  $\sigma$  of graphene and the in-plane electric field via  $\mathbf{K}(\mathbf{k}_{\parallel}, \omega) = \sigma(\mathbf{k}_{\parallel}, \omega)\mathbf{E}_{\parallel}(\mathbf{k}_{\parallel}, \omega)$ .

The TM GPPs are determined by coupling the solutions in each of the dielectric regions via the BCs in Eqs. (1). We assume an electric field in the upper (+) and lower (−) dielectric regions of the form  $\mathbf{E}_{\text{TM}}^{\pm}(\mathbf{r}) = \mathcal{E}_{\text{TM}}^{\pm} \exp(ik_{\parallel}y) \exp(\mp k_{\perp}^{\pm}z)$  where  $k_{\parallel}$  and  $k_{\perp}$  are propagation constants in the parallel and perpendicular directions. They obey  $k_{\parallel}^2 = \varepsilon_{\pm}k_0^2 + (k_{\perp}^{\pm})^2$ , where

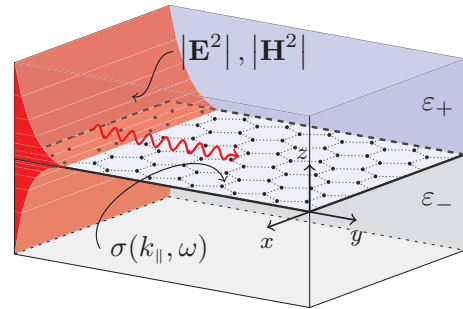


Fig. 1. Schematic illustration of a graphene monolayer, characterized by its conductivity  $\sigma(k_{\parallel}, \omega)$ , sandwiched between two dielectric materials with dielectric constants  $\varepsilon_{\pm}$ .

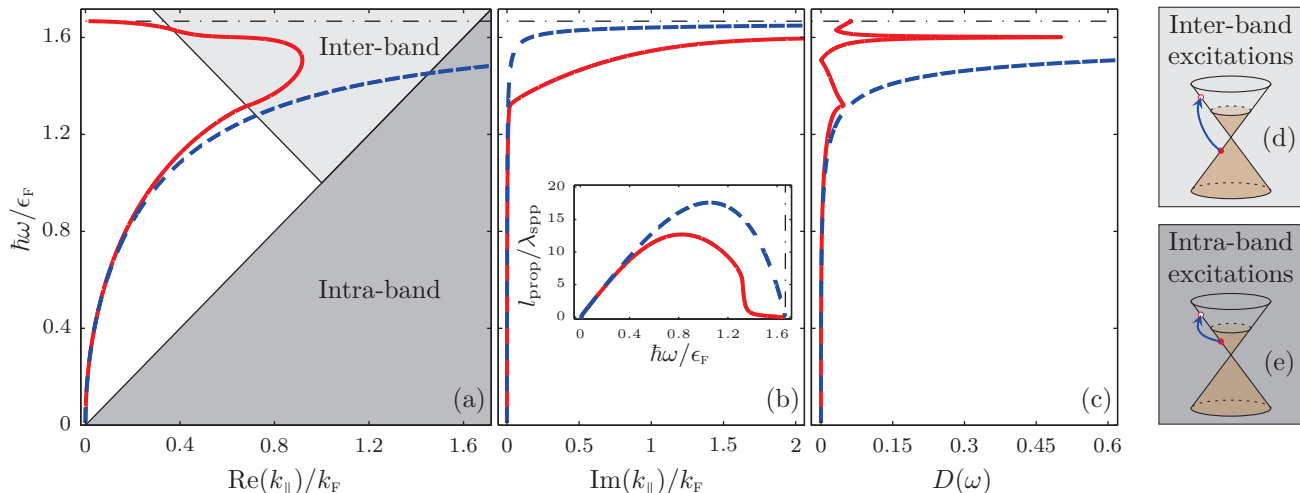


Fig. 2. Dispersion properties of GPP within a nonlocal description (solid lines) and the local-response approximation (dashed lines) for freely suspended graphene ( $\epsilon_{\pm} = 1$ ) with  $\epsilon_F = 1$  eV,  $\tau = 10^{-13}$  s, and  $\hbar\omega_{\text{sp}}/\epsilon_F \approx 1.6671$  (horizontal dash-dotted lines). Panel (a) and (b) show the real and imaginary parts of the complex dispersion relation (inset: the propagation length), while panel (c) shows the corresponding GPP density-of-states. Panels (d) and (e) illustrate the difference between the inter- and intra-band excitations.

$k_0 = \omega/c$  is the free-space propagation constant. The vectors  $\mathcal{E}_{\text{TM}}^{\pm}$  determine the polarization of the field, here assumed TM, such that the  $\mathbf{H}$ -field is polarized along the  $x$ -direction. Thus, the field solutions decay exponentially from the  $z = 0$  plane whilst propagating along the  $y$ -direction. The in-plane propagation constant  $k_{\parallel}$  is then determined by

$$\frac{\epsilon_+}{\sqrt{k_{\parallel}^2 - \epsilon_+ k_0^2}} + \frac{\epsilon_-}{\sqrt{k_{\parallel}^2 - \epsilon_- k_0^2}} = \frac{-4\pi i \sigma(k_{\parallel}, \omega)}{\omega}, \quad (2)$$

where  $\sigma$  is implicitly assumed to depend only on the real part of  $k_{\parallel}$ . The electrostatic approximation  $k_{\parallel} \gg k_0$  leads to a simpler dispersion equation:  $k_{\parallel} = i(\epsilon_+ + \epsilon_-)\omega/[4\pi\sigma(k_{\parallel}, \omega)]$ . This approximate form of the dispersion equation is very accurate for TM modes in doped graphene [4] and will be used throughout this work. From Eq. (2) it is apparent that a necessary condition for the existence of TM GPP is the positivity of the imaginary part of  $\sigma(k_{\parallel}, \omega)$ . The presence of damping, corresponding to nonzero, positive values of the real part of  $\sigma(k_{\parallel}, \omega)$ , induces an imaginary component to the  $k_{\parallel}$ , indicative of a finite life-time of the GPPs.

The conductivity is related to the polarizability  $\chi$  via  $\sigma(k_{\parallel}, \omega) = \frac{ie^2\omega}{k_{\parallel}^2}\chi(k_{\parallel}, \omega)$  [17]. The polarizability of doped graphene within the low-energy Dirac model has previously been derived in the non-interacting limit for real frequencies in Refs. [11, 12] and for complex frequencies in Ref. [8] in the low-temperature limit. Importantly, these results have the full  $k_{\parallel}$ -vector dependence and account fully for the nonlocal plasma response. Previous work on TM GPPs has primarily treated the conductivity in the local-response limit, where  $\sigma(k_{\parallel}, \omega)$  is approximated by  $\sigma(\omega)$ , valid when  $k_{\parallel} \ll k_F$  [18]. The question of the precise range of validity of such local approximations

remains to be thoroughly addressed.

An important concept for mode propagation is the group velocity  $v_g = [\text{Re}(\partial k_{\parallel}/\partial \omega)]^{-1}$ . In a local model without relaxation and at low temperatures, the conductivity is entirely imaginary for  $\hbar\omega < 2\epsilon_F$ . Assuming that the TM GPP exists within this window, the local conductivity can be written as  $\sigma(\omega) = i\sigma_1(\omega)$ , and we get

$$v_g(\omega) = \left( \frac{4\pi}{\epsilon_+ + \epsilon_-} \right) \frac{\sigma_1(\omega)}{1 - \omega \frac{\partial \sigma_1(\omega)}{\partial \omega} / \sigma_1(\omega)}. \quad (3)$$

Associating the surface plasmon frequency  $\omega_{\text{sp}}$  with the singularity where  $v_g(\omega_{\text{sp}}) = 0$ , Eq. (3) implies that  $\omega_{\text{sp}}$  is then solely defined by the zeros of  $\sigma_1(\omega)$ . Thus, in a local-response approximation, the surface plasmon frequency is entirely independent of the dielectric surroundings. We arrive at the same conclusion starting from the full expression in Eq. (2). The primary effect of the surrounding dielectric media is to induce an overall shift of the slope of the polariton branch of the GPP dispersion while the horizontal plasmon branch remains unchanged.

We display various aspects of the local and nonlocal dispersion relations of a GPP guided by a free-standing layer of graphene ( $\epsilon_{\pm} = 1$ ) in Fig. 2. Random scattering is included via a phenomenological relaxation time  $\tau = 1 \times 10^{-13}$  s through Mermin's self-consistent relaxation time approximation [19]. The local and nonlocal results are in excellent agreement for low excitation energies  $\hbar\omega/\epsilon_F \lesssim 1$ . As the dispersion moves into the region  $\hbar\omega/\epsilon_F + \text{Re}(k_{\parallel})/k_F > 2$ , a deviation develops rapidly. The origin of this behavior lies in the available electronic excitations [panels (d) and (e)]. In the local limit, electron excitations cannot carry a momentum change. Consequently, intra-band excitations, Fig. 2(e), are excluded and inter-band excitations must

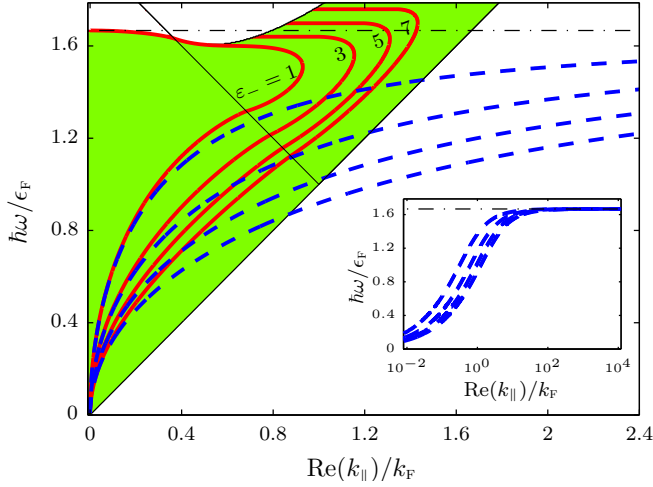


Fig. 3. Dispersion of GPP within a nonlocal (solid lines) and a local-response approximation (dashed lines) for substrate-supported graphene ( $\varepsilon_+ = 1$ ,  $\varepsilon_-$  varies from 1 to 7) with  $\varepsilon_F = 1$  eV and  $\tau \rightarrow \infty$ . The region where  $\text{Im}[\sigma(k_{\parallel}, \omega)] > 0$  is indicated in green. The inset displays the local solutions (logarithmic horizontal axis) emphasizing the substrate-independent divergence at  $\hbar\omega_{\text{sp}}/\varepsilon_F \approx 1.6671$  (dash-dotted line).

be vertical, and they can occur only for  $\hbar\omega > 2\varepsilon_F$ . Conversely, in a nonlocal description excitations can support a momentum change, and excitations need no longer be vertical. Thus, inter-band excitations are possible when  $\hbar\omega/\varepsilon_F + \text{Re}(k_{\parallel})/k_F > 2$  and  $\hbar\omega/\varepsilon_F > \text{Re}(k_{\parallel})/k_F$ . This is the reason behind the qualitative differences between the local-response approximation and a nonlocal description. Furthermore, the nonlocal GPPs are strongly damped by the interband excitations which is reflected in the apparent deviations between local and nonlocal descriptions at higher energies as observed in Fig. 2(a)-(c).

The effects due to substrate dielectric constant in a substrate-graphene-vacuum setup are illustrated in Fig. 3. Within the local description, the dispersion develops a divergence at  $\hbar\omega_{\text{sp}}/\varepsilon_F \approx 1.6671$ , independent of the substrate dielectric constant. Similar conclusions have recently been drawn from ab-initio studies of the longitudinal plasmons in graphene on SiC [20]. This is in stark contrast to TM surface plasmon polaritons supported by a metal-dielectric interface, where the surface plasmon branch scales as  $\omega_{\text{sp}} \propto 1/\sqrt{1+\varepsilon}$  [21], in an apparent contradiction. The nonlocal solutions are qualitatively different from the seemingly innocuous local-response approximations at large frequencies, exemplified by a removal of the divergence near  $\text{Re}(k_{\parallel}) \sim k_F$ , the natural upper momentum-scale set by the doping level. Additionally, the point of vanishing group velocity, corresponding to the surface plasmon frequency  $\omega_{\text{sp}}$ , obtains a notable substrate-dependence. The region where  $\text{Im}[\sigma(k_{\parallel}, \omega)] > 0$  is indicated in Fig. 3 to emphasize a qualitative separation between the local and nonlocal descriptions. In a local description, the conductivity is in-

dependent of  $k_{\parallel}$  and exhibits positive imaginary value in the region  $0 < \hbar\omega/\varepsilon_F \lesssim 1.6671$ . The TM GPP branch is therefor limited to this region. In a nonlocal description, the conductivity exhibits positive imaginary values in a larger  $\omega$ -region due to the presence of a  $k_{\parallel}$ -dependence, allowing the TM GPP branch to exist in an extended  $\omega$ -region.

To summarize: we have discussed the qualitative differences between a local and nonlocal description of the conductivity, essential in a complete discussion of the properties of the TM GPPs. The predictions of the two descriptions differ significantly at higher frequencies, indicating that local descriptions may not necessarily suffice in  $(k_{\parallel}, \omega)$ -regions supporting interband excitations, and should be applied with caution. These results are of importance for future analytical and numerical studies of TM GPPs for optical frequencies  $\hbar\omega$  comparable to the doping level  $\varepsilon_F$ .

*Acknowledgments.* The Center for Nanostructured Graphene is sponsored by the Danish National Research Foundation.

## References

1. R. R. Nair, P. Blake, A. N. Grigorenko, K. S. Novoselov, T. J. Booth, T. Stauber, N. M. R. Peres, and A. K. Geim, *Science* **320**, 1308 (2008).
2. F. Bonaccorso, Z. Sun, T. Hasan, and A. C. Ferrari, *Nature Photonics* **4**, 611 (2010).
3. Q. Bao and K. P. Loh, *ACS Nano* **6**, 3677 (2012).
4. F. H. L. Koppens, D. E. Chang, and F. J. García de Abajo, *Nano Letters* **11**, 3370 (2011).
5. Y. V. Bludov, M. I. Vasilevskiy, and N. M. R. Peres, *EPL* **92** (2010).
6. M. Jablan, H. Buljan, and M. Soljačić, *Opt. Express* **19**, 11236 (2011).
7. A. Y. Nikitin, F. Guinea, F. J. García-Vidal, and L. Martín-Moreno, *Phys. Rev. B* **84**, 195446 (2011).
8. B. E. Sernelius, *Phys. Rev. B* **85**, 195427 (2012).
9. B. K. Daas, K. M. Daniels, T. S. Sudarshan, and M. V. S. Chandrashekar, *Journal of Applied Physics* **110** (2011).
10. S. A. Mikhailov and K. Ziegler, *Phys. Rev. Lett.* **99**, 016803 (2007).
11. B. Wunsch, T. Stauber, F. Sols, and F. Guinea, *New Journal of Physics* **8**, 318 (2006).
12. E. H. Hwang and S. Das Sarma, *Phys. Rev. B* **75**, 205418 (2007).
13. S. Raza, G. Toscano, A.-P. Jauho, M. Wubs, and N. A. Mortensen, *Phys. Rev. B* **84**, 121412(R) (2011).
14. G. Toscano, S. Raza, A.-P. Jauho, N. A. Mortensen, and M. Wubs, *Opt. Express* **20**, 4176 (2012).
15. G. Toscano, S. Raza, S. Xiao, M. Wubs, A.-P. Jauho, S. I. Bozhevolnyi, and N. A. Mortensen, *Opt. Lett.* **37**, 2538 (2012).
16. W. Yan, M. Wubs, and N. A. Mortensen arXiv:1204.5413.
17. H. Bruus and K. Flensberg, *Many-body Quantum Theory In Condensed Matter Physics: An Introduction* (Oxford University Press, 2004).

18. L. A. Falkovsky and A. A. Varlamov, *European Physical Journal B* **56**, 281 (2007).
19. N. D. Mermin, *Phys. Rev. B* **1**, 2362 (1970).
20. J. Yan, K. S. Thygesen, and K. W. Jacobsen, *Phys. Rev. Lett.* **106**, 146803 (2011).
21. S. A. Maier, *Plasmonics: Fundamentals and Applications* (Springer, 2007), 1st ed.